

Surface motion of mountain glaciers derived from satellite optical imagery

E. Berthier^{a,*}, H. Vadon^b, D. Baratoux^c, Y. Arnaud^d, C. Vincent^e,
K. L. Feigl^c, F. Rémy^a, B. Legrésy^a

^aLEGO/CNRS/UPS, 18 av. Ed. Belin, 31401, Toulouse Cedex 9, France

^bCNES, 18 av. Ed. Belin, 31401, Toulouse Cedex 9, France

^cLDTP/CNRS/UPS, 14 av. Ed. Belin, 31400, Toulouse, France

^dGREAT ICE (IRD) 54 Rue Molière, BP 96, 38402 St Martin d'Hères, France

^eLGGE (UJF-CNRS) 54 Rue Molière, BP 96, 38402 St Martin d'Hères, France

Received 21 June 2004; received in revised form 21 September 2004; accepted 3 November 2004

Abstract

A complete and detailed map of the ice-velocity field on mountain glaciers is obtained by cross-correlating SPOT5 optical images. This approach offers an alternative to SAR interferometry, because no present or planned RADAR satellite mission provides data with a temporal separation short enough to derive the displacements of glaciers. The methodology presented in this study does not require ground control points (GCPs). The key step is a precise relative orientation of the two images obtained by adjusting the stereo model of one “slave” image assuming that the other “master” image is well georeferenced. It is performed with numerous precisely-located homologous points extracted automatically. The strong ablation occurring during summer time on the glaciers requires a correction to obtain unbiased displacements. The accuracy of our measurement is assessed based on a comparison with nearly simultaneous differential GPS surveys performed on two glaciers of the Mont Blanc area (Alps). If the images have similar incidence angles and correlate well, the accuracy is on the order of 0.5 m, or 1/5 of the pixel size. Similar results are also obtained without GCPs. An acceleration event, observed in early August for the *Mer de Glace* glacier, is interpreted in term of an increase in basal sliding. Our methodology, applied to SPOT5 images, can potentially be used to derive the displacements of the Earth's surface caused by landslides, earthquakes, and volcanoes.

© 2004 Elsevier Inc. All rights reserved.

PACS: 92.40.V; 07.87; 06.30.B

Keywords: Mountain glaciers; Surface displacement; SPOT5; Cross-correlation; Satellite optical images

1. Introduction

Accurate displacement measurements are needed to understand the dynamics of glaciers. Such measurements contribute to a better knowledge of the rheological parameters controlling the flow of glaciers. They are important to monitor icefalls, glacier surges (Fischer et al., 2003), and glacier hazards (Kääb et al., 2003). They can also detect ice-velocity changes caused by global warming (Rignot et al., 2002). Differential Global Positioning System (DGPS) ground surveys, synthetic aperture radar interferometry (InSAR), and optical image cross-correlation are the

main ways to determine glacier displacements. The first two methods are the most accurate but present some severe limitations for the monitoring of mountain glaciers, i.e. all glaciers except large ice caps, ice fields, and the Greenland and Antarctic ice sheets. This study applies cross-correlation to well coregistered SPOT5 optical images to measure mountain glacier surface velocities.

Even with the advent of the DGPS, it remains difficult and time-consuming to perform regular ground-based surveys of glacier flow. Among the 86 regularly monitored glaciers with time series longer than 10 years (Braithwaite, 2002), only a few stakes on the flat parts can reasonably be surveyed, excluding icefalls and remote glaciers.

The 1990s brought some great improvements in the measurement of the surface motion of glaciers from satellite

* Corresponding author. Tel.: +33 5 6133 3017.

E-mail address: etienne.berthier@cnes.fr (E. Berthier).

data. Two new techniques have been extensively investigated, especially on the rapid and large ice streams draining the Antarctic and Greenland ice sheets: InSAR and feature-tracking on optical images.

Combining two SAR images of the Rutford Ice Stream with short time separation (6 days), Goldstein et al. (1993) used InSAR to measure the flow of ice streams. Basic InSAR only measures the projection of the displacement vector onto the satellite line of sight. However, combining ascending and descending passes of the satellite and adding constraints on the ice flow yields all three components of the displacement vector (Joughin et al., 1998; Mohr et al., 1998). Recently, intensity-tracking and coherence-tracking, two cross-correlation techniques applied to SAR data, have been combined with InSAR to produce two-dimensional velocity fields (Gray et al., 2001; Strozzi et al., 2002).

If the correlation between the two radar images is good and the tropospheric, orbital, and topographic contributions can be modelled, the precision of InSAR is on the order of a centimeter (Massonnet & Feigl, 1998). However, additional errors may arise in resolving the phase ambiguity through unwrapping, especially in areas where the displacement gradient (i.e. strain) approaches the threshold of about 10^{-3} for ERS (Massonnet & Feigl, 1998). This condition often occurs in icefalls or marginal shear zones of glaciers (Goldstein et al., 1993).

On mountain glaciers, only a few studies (Mattar et al., 1998; Rabus & Fatland, 2000; Strozzi et al., 2002) have succeeded in measuring motion with InSAR. The steep topography, the strong tropospheric contribution, and the small size of the glaciers are obstacles to overcome. But the major problem is the time between two successive images. If it exceeds 1 or 3 days (Strozzi et al., 2002), the displacement gradient is larger than the threshold (10^{-3} for ERS), destroying the interferometric fringes. Furthermore, after a few days, the correlation is low due to rapid changes on the glacier surface. Only the ERS-1 ice phase (3-day orbital cycle) and the ERS-1 and ERS-2 Tandem Mission (1 day separating the passes of the satellites) can be used to derive velocity fields on glaciers. Consequently, no present or planned satellite mission can measure the motion of mountain glaciers using InSAR.

Repeated visible or near infrared images of the same area can be used to track the displacement of features such as crevasses or surficial debris moving with the ice (Lucchitta & Ferguson, 1986). Development of automatic feature-tracking algorithms has substantially increased the accuracy and the efficiency of this approach (Scambos et al., 1992).

The aim of our study is to demonstrate that high-resolution and accurate surface displacement maps can be routinely obtained on mountain glaciers using optical images. The goal is to provide an alternative to InSAR for the measurement of the glacier flow.

Correlation of optical images provides the two horizontal components of the displacement vector contrary to InSAR. Furthermore, the measurement is unambiguous: absolute

displacements can be referenced to motionless areas which are always available for mountain glaciers. This approach can be applied to images with a large time separation. For some outlet glaciers of Greenland or Antarctic ice sheets, the persistence of the surface features permits velocity measurements from images separated by as much as 11 years (Berthier et al., 2003). Some velocity fields have also been derived from optical images separated by more than a year on mountain glaciers (e.g., Kääb, 2002). Previous studies on Antarctic ice streams (Scambos et al., 1992; Frezzotti et al., 1998) or mountain glaciers (Kääb, 2002) generally reached an accuracy of ± 1 pixel. A smaller uncertainty and a methodology adapted to mountain glaciers are the focus of our study.

In the next section, we describe a procedure to extract displacements of the ground surface from two SPOT5 images. The images and the different data needed to apply and validate our methodology are presented for the Mont Blanc area in Section 3. Maps of the satellite-derived displacements and accuracy of our measurements are presented in Section 4. An acceleration event of the *Mer de Glace* glacier is also discussed before presenting conclusions.

2. Methodology

Even slightly different incidence angles can create a relative distortion between two satellite images of the same area. If the two images are correlated, the resulting offsets in the image lines and columns are the sums of the contributions from misregistration, topography, orbits, and attitude as well as the glacier-dynamics signal. To obtain a valid measurement, we must remove all the contributions except the glacier flow. The principle of our method is to resample one of the images (called the “slave” image) in the native (1A) geometry of the other, “master” image just as for InSAR (Massonnet & Feigl, 1998). To do this, we use an accurate stereoscopic model (called stereo model in the following), a digital elevation model (DEM), and an interpolator that respects the Shannon criteria. The two images can then be correlated to estimate the deformation of the glaciers. Fig. 1 presents all the steps required to measure glacier-surface displacement from two satellite images. All the algorithms describing the SPOT5 stereo model and used in this study are the property of the Centre National d'Etude Spatial (CNES). The information needed to perform these calculations are available in a handbook (SPOT-Image, 2002), available upon request to the SPOT-Image company.

2.1. Characteristics of mountain glaciers and required accuracy

The time separation between images is one of the critical factors for a reliable measurement. It must be long enough to increase the signal (the flow of the glaciers) but short

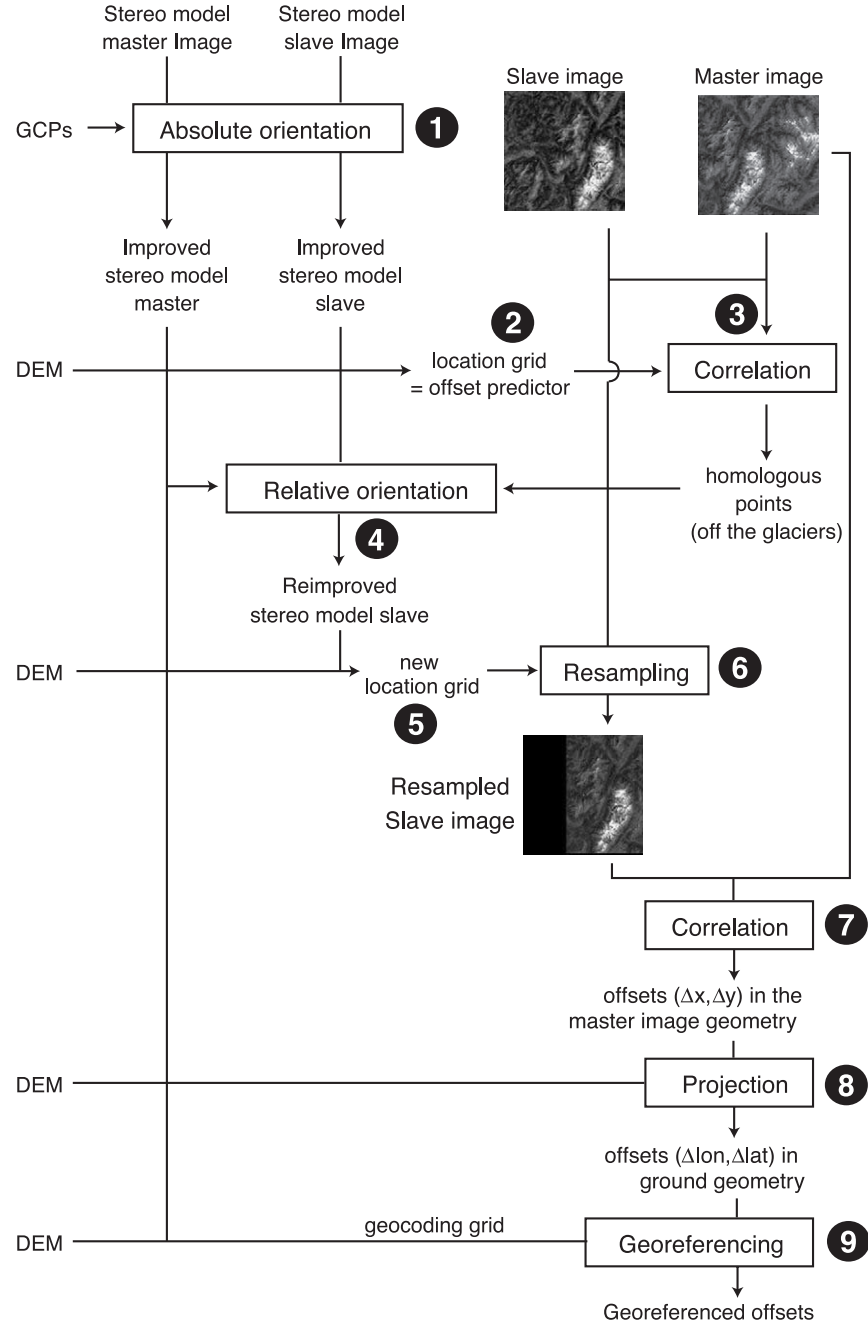


Fig. 1. Flowchart of the methodology followed to measure the surface displacements from two SPOT5 images. On the left side, GCPs (ground control points) and DEM (digital elevation model) represent external informations.

enough to preserve the features for tracking. Indeed, for many mountain glaciers, a long time separation will reduce the efficacy of the cross-correlation for two reasons.

First, the surface features of the glaciers may change due to melting of snow cover or ice, snowfall or changes caused by windblown snow. Correlation between the two images breaks down and only sparse measurements can be obtained.

Second, good features for the correlation such as the crevasses and the Forbes bands, appear from year to year at the same places with similar shapes, like river eddies. For

example, crevasses open regularly upstream of an icefall. We tested that correlating two images 1 year apart on the *Mer de Glace* glacier can lead to an (incorrect) null displacement in some parts of the glacier. For shorter times, the spatial continuity of the displacement field prevents this problem.

Studying a glacier flowing at 75 m a^{-1} with images separated by 1 month, we seek to detect a displacement of 6.25 m . A reasonable accuracy is obtained if the error does not exceed 0.62 m (10%). Using SPOT5 images with a pixel size of 2.5 m , we will achieve this goal if the uncertainty is $\pm 0.25 \text{ pixels}$, four times better than previously reported. In

previous studies, the uncertainties resulted mainly from the difficulty of coregistering and removing the topographic distortion between the two images. These two issues are addressed thoroughly in our methodology.

2.2. Absolute orientation (step 1 in Fig. 1)

Ground control points (GCPs) are identifiable with an accuracy of ± 1 pixel on both images. They also have known geographic coordinates. They improve the stereo model and consequently the georeferencing of both master and slave images. The stereo model, including the position and the attitude of the satellite, determines the correct ground position of each point in the image (Toutin & Cheng, 2002). The stereo model is computed with an iterative least-squares bundle block adjustment. Estimates of the attitude (roll, pitch, and yaw) and the focal length of the sensor are provided with the images. From n GCPs, we estimate a new attitude and focal length which minimizes the function:

$$\sum_{i=1}^n \|\overrightarrow{G_i G'_i}\|^2 \quad (1)$$

where $G_i = (\lambda, \phi, z)_i$ is the exact position of the i th GCP and $G'_i = (\lambda', \phi, z')_i$ its ground position deduced from its image coordinates using the stereo model. λ, ϕ, z represent the latitude, longitude, and ellipsoidal height. A rigorous satellite stereo model is more accurate than a simple, polynomial-based model (Toutin & Cheng, 2002). For areas with rugged topography, a polynomial does not suffice to accurately model the stereoscopic distortions between images. A rigorous model also takes advantage of the SPOT5 satellite products which include a precise description of the orbit and attitude.

After this step, each point on the images can be located on the ground with an accuracy of ± 2.5 m (one pixel) or slightly better.

2.3. Relative orientation (step 2 to 4 in Fig. 1)

Without GCPs, this relative orientation is the only way to obtain well coregistered images. Even if GCPs are available, this step will improve the coregistration because it uses numerous and accurate homologous points. It yields two images coregistered within a few tenths of a pixel. It improves the stereo model of the slave image only, by assuming that the master image is now perfectly georeferenced.

The motionless homologous points are identified by cross-correlating the two images. The automatic extraction of homologous points is difficult directly because the same feature can be separated by as many as a thousand pixels between the two images. Instead, we first compute a location grid using the stereo models of the two images and a DEM. This grid provides the rough offset separating a

pixel of the slave image from its corresponding pixel in the master image. It is used as a first estimate (or an offset predictor) to correlate the master and the slave image. Using a mask which excludes all the glaciers, we then compute the correlation only on the motionless areas of the images (step 3). Retaining only the points with the best correlation, we create a set of accurate homologous points distributed throughout the images.

The homologous points are used to improve the stereo model of the slave image only (step 4). It yields new values of the attitude (roll, pitch, and yaw) and focal length.

2.4. Resampling of the slave image (steps 5 and 6 in Fig. 1)

The objective of this step is to project the slave image into the geometry of the master image so that the remaining offsets represent only the deformation of the Earth's surface.

The stereo models of the two images are combined with a DEM to create a new, more precise, location grid in step 5. This grid contains the orbital, attitude, and topographic contributions to the total offsets between the two images. It is used to create a resampled slave image in step 6, as if it had been acquired from exactly the same viewpoint as the master image. We use a resampling method which respects the Shannon criteria to preserve the radiometry and to minimize aliasing. As in Vadon and Massonnet (2000), we apply an apodized cardinal sine (cardinal sine multiplied by a Gaussian function) for interpolation. It is the best compromise between the Shannon criteria requirement and the filter length. It also leads to lower bias than other interpolators (Van Puymbroeck et al., 2000).

2.5. Cross correlation (step 7 in Fig. 1)

Now that they share the same geometry, the two images are correlated to estimate the offsets (step 7). We use the MEDICIS correlator software, developed at CNES and commercially available (Centre National d'Etude Spatiale, 2002). For SPOT5 images, the accuracy of the correlation itself is expected to be on the order of a few hundredths of a pixel. Surface changes and radiometric differences caused by different incidence and/or solar illumination angles are the limiting factors for the correlation.

At each grid point, the offsets between the two images are deduced from the position of the maximum of the correlation. This maximum is found in an iterative process. On subscenes of 21 by 21 pixels (or 52.5 by 52.5 m for SPOT5 images), we compute the correlation coefficient between the master and a shifted slave image. The sub-pixel shift is applied to the slave image with a cardinal sine interpolator. It is more accurate than simple interpolation of the correlation coefficient grid calculated for every pixel (Vadon & Massonnet, 2000).

With correlation windows of 21×21 pixels, a posting of 10 pixels (25 m) captures the fine details of the ice flow. The correlation leads to two offset fields: offsets in the image

column direction (Δx) and line direction (Δy). The correlation coefficient helps to assess the quality of the measurement.

2.6. Extracting ground displacements (steps 8 and 9 in Fig. 1)

The offsets measured between the two images represent the projection of the displacement vector onto the plane of the master image. These offsets can be used either in the native image geometry or transformed to displacements in latitude and longitude. Usually, offsets in pixels are simply converted to displacements in meters multiplying by a constant value for the pixel size (2.5 m for SPOT5). This is an approximation in areas with rugged topography. In the glacial areas in our images, the ground distance contained within a pixel ranges from 2.5 to 3 m in the line direction and from 2.5 to over 10 m in the column direction. It is even larger on the steep slopes surrounding the glaciers.

Fig. 2 illustrates the conversion from image offsets to ground displacements. The master image stereo model and the DEM are used to compute the corresponding location on the ground ((λ_m, ϕ_m, z_m)) for each pixel of the master image ((x, y)). When the slave image is acquired, the pixel has moved to a new position ($(x + \Delta x, y + \Delta y)$) measured by the cross-correlation. Using the same transformation, we compute the new location ((λ_s, ϕ_s, z_s)) of this point on the ground. We then deduce the displacements in latitude $\Delta\phi$ and longitude $\Delta\lambda$ and the total horizontal displacement. A value of the change in altitude (Δz) of the point is also obtained. This is not a measurement of the vertical component of the displacement vector because of ice ablation and the ice flow direction that is not exactly parallel to the surface (Paterson, 1994).

Now, we know the displacements in latitude and longitude every 10 pixels of the master image. In step 9, we map them into a geographic reference system using a georeferencing grid calculated with the master image stereo

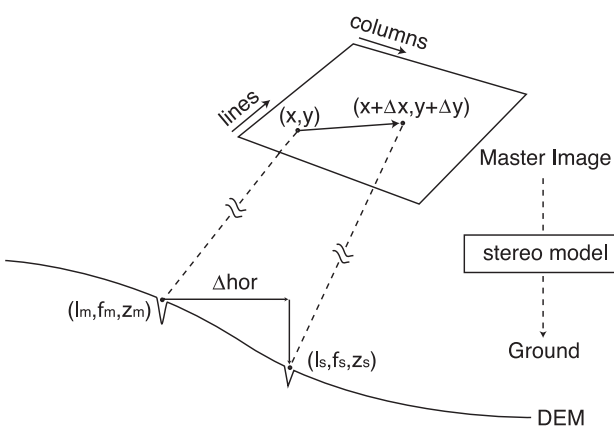


Fig. 2. Conversion of offsets in master image geometry to georeferenced ground displacements.

Table 1

Characteristics of the four SPOT5 images used in this study

Date (2003)	ID	Incid. angle
19 Jul	50512570307191024221B0	-23.6
19 Aug	50522570308191028122B4	-15.2
23 Aug	50512570308231051191B0	+15.7
18 Sep	50522570309181051081B3	+17.3

The image pairs (19 Jul/19 Aug 2003) and (23 Aug/18 Sep 2003) are used to measure the displacements of the glaciers in 31 and 26 days, respectively. The 19 Aug/23 Aug 2003 pair is used to compute a DEM of the Mont Blanc area. Note that the incidence angle refers to the center of the images.

model and the DEM. This grid is then used to project the offsets. The resampling is also performed using an apodized cardinal sine.

3. Study area and available data

In this section, we describe the data used to test and validate our methodology on glaciers of the Mont Blanc area. The two largest glaciers of this mountain range, the *Mer de Glace* and *Argentière* glaciers have been studied for more than a century (Reynaud, 1980). Their accessibility facilitates the field campaigns for verification of satellite-derived measurements.

3.1. SPOT-5 images of the Mont Blanc area

The SPOT5 satellite was launched on 4 May 2002 with a repeat-orbital cycle of 26 days. The ground resolution has been improved with a pixel size of 2.5 m in THR mode (compared to 10 m for SPOT1-4), while retaining an area footprint on the ground of 60×0 km. Precise orbital ephemeris and attitude descriptions are provided with the images. Without any ground control points, an image is located on the ground with a precision of 30 m rms. A detailed description of the SPOT5 mission can be found in Fratter et al. (2001).

Four SPOT5 images of the Mont Blanc area were acquired during the summer of 2003 (Table 1). The time of acquisition of the images is crucial. Acquiring images during the dry season (July to September in the French Alps), 1 or 2 months apart seems the best compromise. Before July, the snowline is still at a low elevation and the snow cover from the previous winter still masks the surface features. After September, snowfalls can occur at low elevation and dramatically increase the albedo of the glacier. The main displacement field is derived from the images acquired on 23 August and 18 September 2003 (named image pair #2 in the following). In Fig. 3, the outlines of these two images are plotted on a DEM of the area. Separated by one orbital cycle, they have similar viewpoints. The small difference in the incidence angles at the center of the images (Table 1) is explained by their different footprints. The images acquired on 19 July and

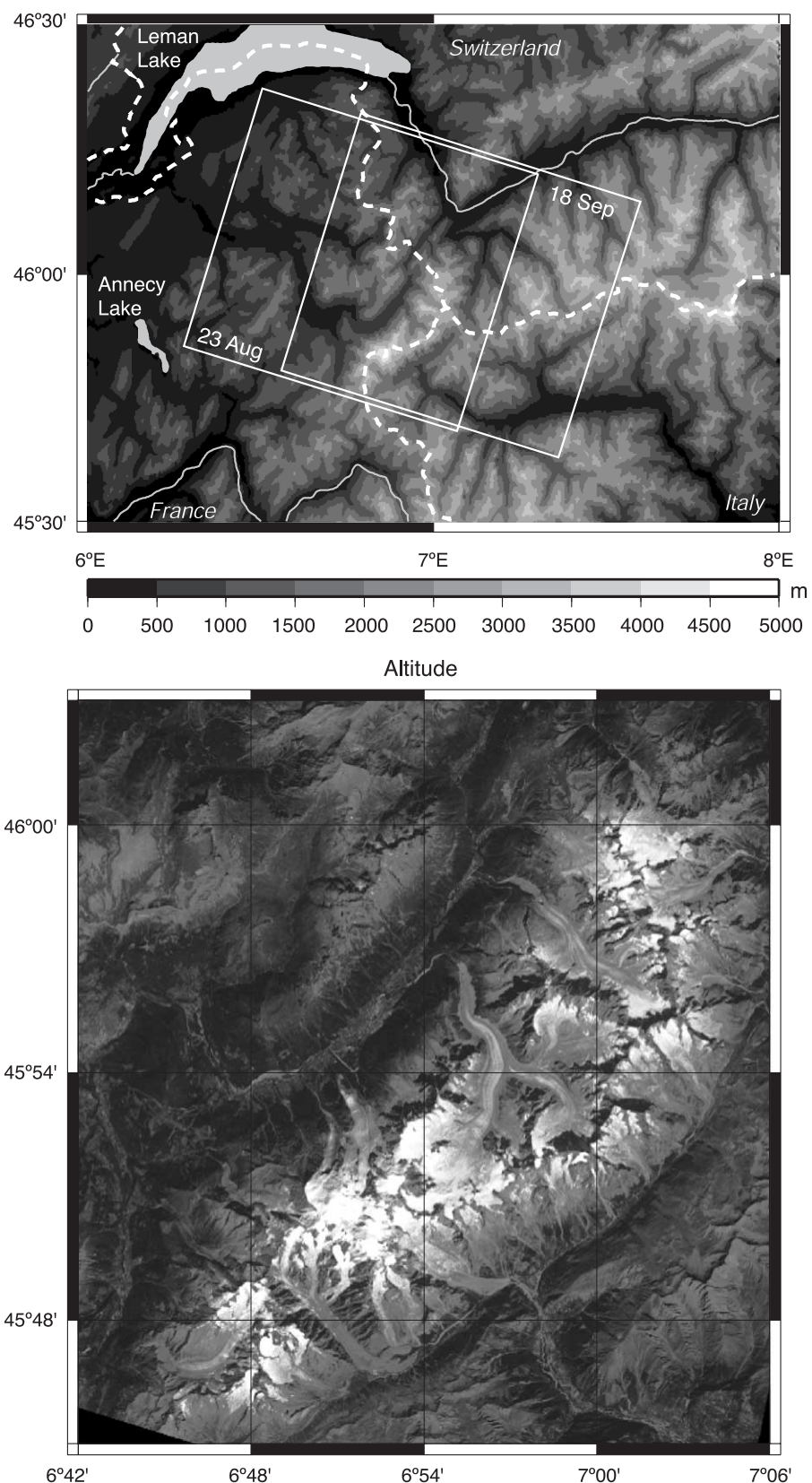


Fig. 3. Outlines of the SPOT5 scenes (23 August 2003 and 18 September 2003) used to derive the main velocity field (upper panel). The background image is the high-resolution DEM used in this study. The lower panel is a subscene of the 23 August 2003 image showing the Mont Blanc area.

19 August 2003 (image pair #1) are also combined to estimate the displacement during 31 days. This pair is used to test a less favourable satellite configuration (with a difference of 8.5° in the incidence angles) and to determine whether the glaciers can experience short-term velocity change.

All these images were acquired with the lowest possible gain. A low gain avoids radiometric saturation on the glacier, especially in the bright snow-covered accumulation area (Ferrigno & Williams, 1983). Level 1A imagery is used to avoid any radiometric and geometric resampling of the data. This level ensures better control of the image geometry (Al-Rousan et al., 1997).

3.2. Digital elevation model (DEM)

To model and remove the stereoscopic distortions between two images, a DEM is needed. Because mountain glaciers in the Mont Blanc area are experiencing rapid thinning (Berthier et al., 2004), a DEM referring to an epoch as near in time as possible to the acquisition date of the satellite images seems preferable. The SPOT5 images acquired on 19 and 23 August 2003 with opposite incidence angles and a short time separation (Table 1) were combined to compute a fine resolution DEM of the area, with a posting of 20 m. The DEM was produced using the Orthoengine module of the PCI-Geomatica software (Toutin & Cheng, 2002). The accuracy of this DEM was tested with 48 independent check-points on the slopes surrounding the glaciers. The mean difference between the SPOT5 DEM and the check-points is 2.5 m ($\sigma=10$ m), the DEM being slightly lower. On the flat surface of the *Mer de Glace* and Argentière glaciers, this difference is only 0.15 m ($\sigma=1.1$ m). Because of shadowing, clouds and the difference in areal coverage, this DEM does not encompass the entire area of interest. A complete DEM is needed and obtained using the SRTM DEM (Rabus et al., 2003) and another SPOT DEM available for 2000. The coarse GTOPO30 DEM (USGS, 1996) was also used to prove that accurate

displacements can be derived without any precise, contemporaneous DEM.

3.3. Ground control points (GCPs)

Some GCPs are preferable to improve the absolute georeferencing of the four SPOT5 scenes. They have been acquired in September and October 2003 with an ASH-TECH single-frequency differential GPS (DGPS) system. The accuracy of these GCP positions is on the order of 0.5 m horizontally and 1 m vertically. They are used in the absolute orientation of the images (step 1). During the computation of the stereo model, the least reliable GCPs are excluded. Table 2 provides some statistics on the GCPs retained. For the different SPOT5 images, the same set of GCPs leads to slightly different residuals ranging from 1.55 to 2.55 m. Table 2 also shows the results of the relative orientation for the different pairs of images (last column). For image pair #2, the orientation is greatly improved. For this pair, the relative orientation is also accurate without GCPs, even when using the less precise GTOPO30 DEM. For image pair #1, the relative orientation does not lead to any improvement because of the less favourable satellite configuration. The significant 8.5° difference in the incidence angles of the two images in pair #1 also explains why the relative orientation is inaccurate without GCPs, even with a precise DEM.

3.4. DGPS measurements of the glacier displacement

Measurement of glacier displacements from satellite images are rarely compared to field measurements because it is difficult to be on the glaciers during the exact time of acquisition of satellite images. Two DGPS field campaigns were planned on the *Mer de Glace* and Argentière glaciers in August and September 2003 to measure the surface displacements. Because of possible cloud cover and the satellite schedule, the acquisition dates of the SPOT5 images could not be known precisely in advance. Con-

Table 2

Standard deviation of the residuals (meters) for the absolute and relative orientation of the different SPOT5 scenes

Image pair	Date (2003)	Abs. orient.		Rel. orient.	
		σ	Max. residual	σ	Max. residual
#1 with GCPs; HR DEM	19 Jul	2.55	4.3	2.84	11.1
	19 Aug	1.89	3.59		
#1 no GCPs; HR DEM	19 Jul/19 Aug	—	—	5.45	31.7
#1 no GCPs; LR DEM	19 Jul/19 Aug	—	—	14.5	38.8
#2 with GCPs; HR DEM	23 Aug	1.55	2.66	0.63	1.45
	18 Sep	1.82	2.97		
#2 no GCPs; HR DEM	23 Aug/18 Sep	—	—	0.67	1.68
#2 no GCPs; LR DEM	23 Aug/18 Sep	—	—	0.67	1.68

For each image, the absolute orientation is computed from ground control points (GCPs). The relative orientation is based on homologous points extracted by cross-correlation of the two images and does not necessarily require an absolute orientation beforehand. The maximum residual for the GCPs (respectively homologous points) retained in the absolute (resp. relative) orientation is also given. HR refers to the high resolution (20 m) DEM and LR to the low resolution (1 km) GTOPO30 DEM.

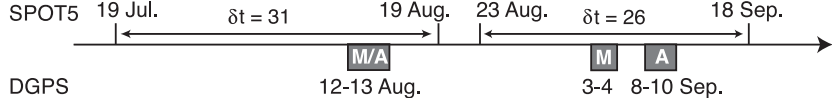


Fig. 4. Comparison between the acquisition times of the SPOT5 images and the DGPS surveys of the glaciers displacements. For the DGPS survey, M refers to the *Mer de Glace* glacier, A to the *Argentière* Glacier.

sequently, the ground surveys were not performed exactly at the same time (Fig. 4). A Leica dual-frequency GPS was used to survey the two successive positions of 29 ablation stakes and painted stones on the glaciers. The precision of the positioning itself is on the order of a few centimeters. The main uncertainty results from the difficulty in placing the GPS antenna exactly at the same position relative to the stakes (a puddle of water usually surrounds each stake in summer-time). Consequently, the uncertainty is 15 cm for a single measurement, leading to a displacement accuracy of ± 21 cm. For painted stones, the uncertainty is larger, but difficult to estimate because they can move or roll independently of the underlying ice.

4. Results

4.1. Map of the displacements in the Mont Blanc area

Fig. 5 shows the horizontal displacement of the ground surface in the Mont Blanc area derived from image pair #2. On these glaciers, no overall velocity measurements had ever been performed. The highest speed occurs on the steep icefalls of the *Mer de Glace*, *Bosson* and *Brenva* glaciers, with velocities over 500 m a^{-1} . Some small-scale features of the displacement field also appear clearly. For example, the increase in velocity of the *Mer de Glace* glacier near the confluence with the *Leschaux* glacier is visible in Fig. 5d. Some problems also appear. No displacements can be measured for areas in shadows; e.g., on the upper part of the *Leschaux* glacier under the steep north face of the *Grandes Jorasses*. At high elevation on the accumulation zone, even with a low gain, the noise remains noticeable.

4.2. Residuals in the unglacierized area

The accuracy of the velocities can be first assessed by a null test over motionless, ice-free areas of the images. We retain only the points with a correlation coefficient over 0.7. Fig. 6 shows the histograms of the residuals (in meters) in the image line direction for image pair #2. As expected, the stronger the correlation coefficient, the smaller the scatter. If the correlation coefficient is greater than 0.95, the uncertainty (noted σ) is 1.8 m whereas $\sigma=6.6$ m if the correlation coefficient is smaller than 0.75. Unexpectedly, the histograms are not exactly centered on 0. Furthermore, the weaker the correlation coefficient, the more negative the average residual (bias) in the line direction.

We suggest that the change in solar illumination angle explains this bias (Fig. 7). Between the two acquisition dates, the Sun has moved, changing the orientation and length of its shadows. The apparent displacement of the shadows is negative and oriented mainly parallel to image lines. The strength of the correlation is weakened by a secondary correlation peak due to the shifted shadows. The larger the shadow, the larger the shift between the two dates and the weaker the correlation coefficient. We verify this hypothesis by comparing the residuals off the glaciers in the image line direction for two different slopes. The southeast-facing slopes, oriented toward the Sun at 9:00 AM local solar time (when the satellite images were acquired), present short shadows and, consequently, have high correlation coefficients and small residuals. The northwest-facing slopes, where the shadows are large, present low correlation coefficient and strong, negative residuals in the line direction.

However, on the glaciers, this “shadowing effect” does not cause a systematic error in our measurements. Shadows are only created by the surficial debris and the surrounding mountains. The best way to ensure a limited bias is to retain only the measurements with the highest correlation coefficient. The effect could be larger for other applications such as landslides, especially if images are acquired during different seasons.

Table 3 gives the offsets off the glaciers for both image pairs in column and line directions. The “shadowing effect” also affects the residuals in lines for image pair #1, but the effect is small because the illumination angle of the Sun did not change much between the two images. In both directions, the standard deviation is larger for pair #1 than for pair #2 because of the difference in the incidence angles of the two images (Table 1). Even with a precise DEM, the distortions between the images could not be perfectly modelled and suppressed.

Our images were acquired for glaciological purposes with a low gain: digital numbers are ranging from 10 to 30 off the glaciers and from 30 to 200 on the glaciers. Consequently, the strength of the correlation peak is much larger on the glaciers. It is thus difficult to transpose readily the uncertainties estimated on the steep slopes surrounding the glaciers to the glaciers. Only DGPS observations can provide a precise estimation of the accuracy of our method.

4.3. Comparison with DGPS displacements

To cover the same length of time, the satellite-derived displacements (occurring in 26 or 31 days) and the DGPS

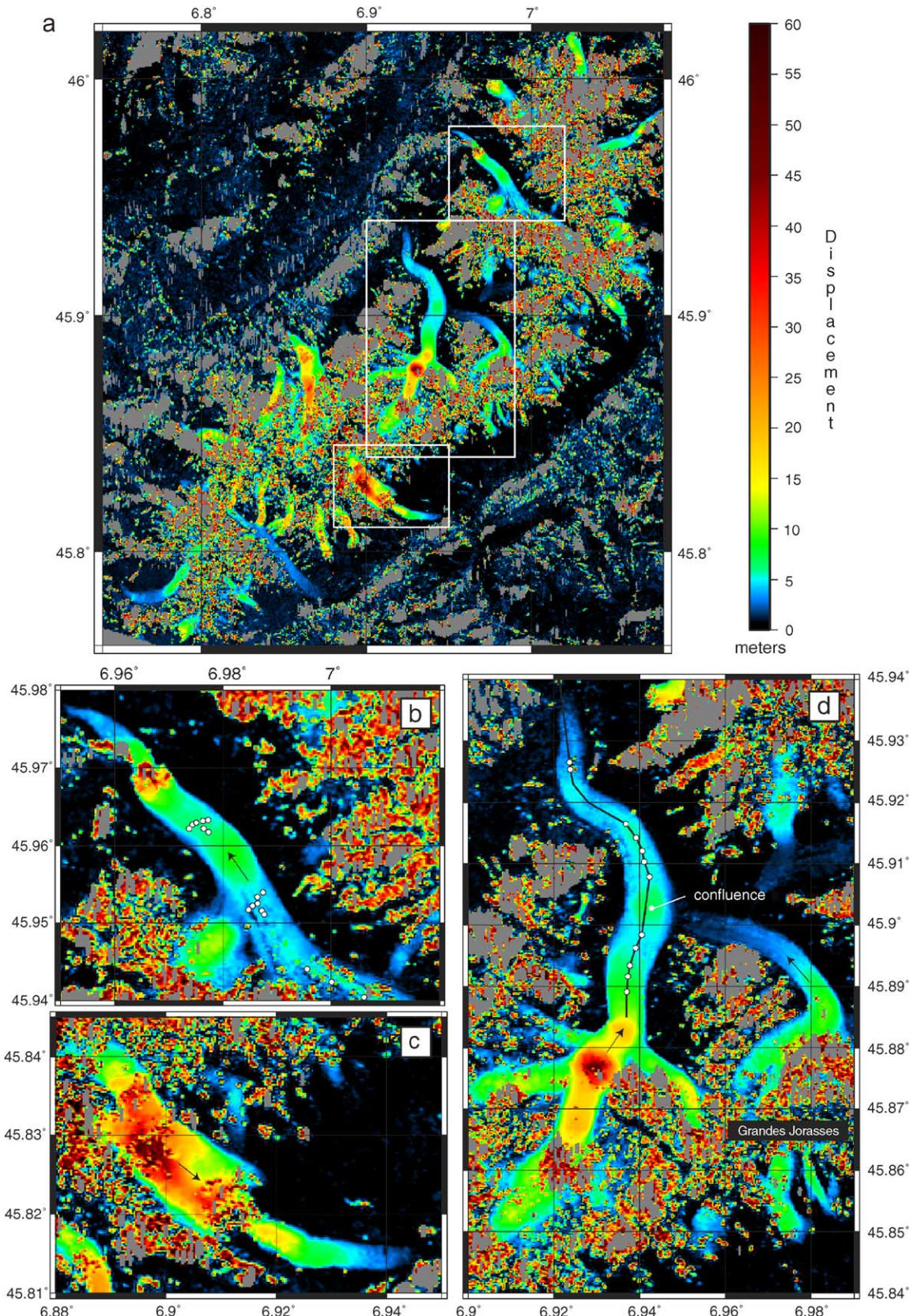


Fig. 5. Horizontal displacement of glaciers of the Mont Blanc area between the 23 August and 18 September 2003 (26 days). The upper panel (a) shows the entire Mont Blanc area. The white outlines encompass the *Argentière*, *Brenva*, and *Mer de Glace* glaciers shown in the three lower panels (b, c, and d), respectively. Where the correlation coefficient is too weak, pixels appear in grey. The white dots are the ablation stakes measured by DGPS. The black line is the longitudinal profile on the *Mer de Glace* glacier shown in Fig. 8. The black arrows in the three lower panels indicate the direction of flow.

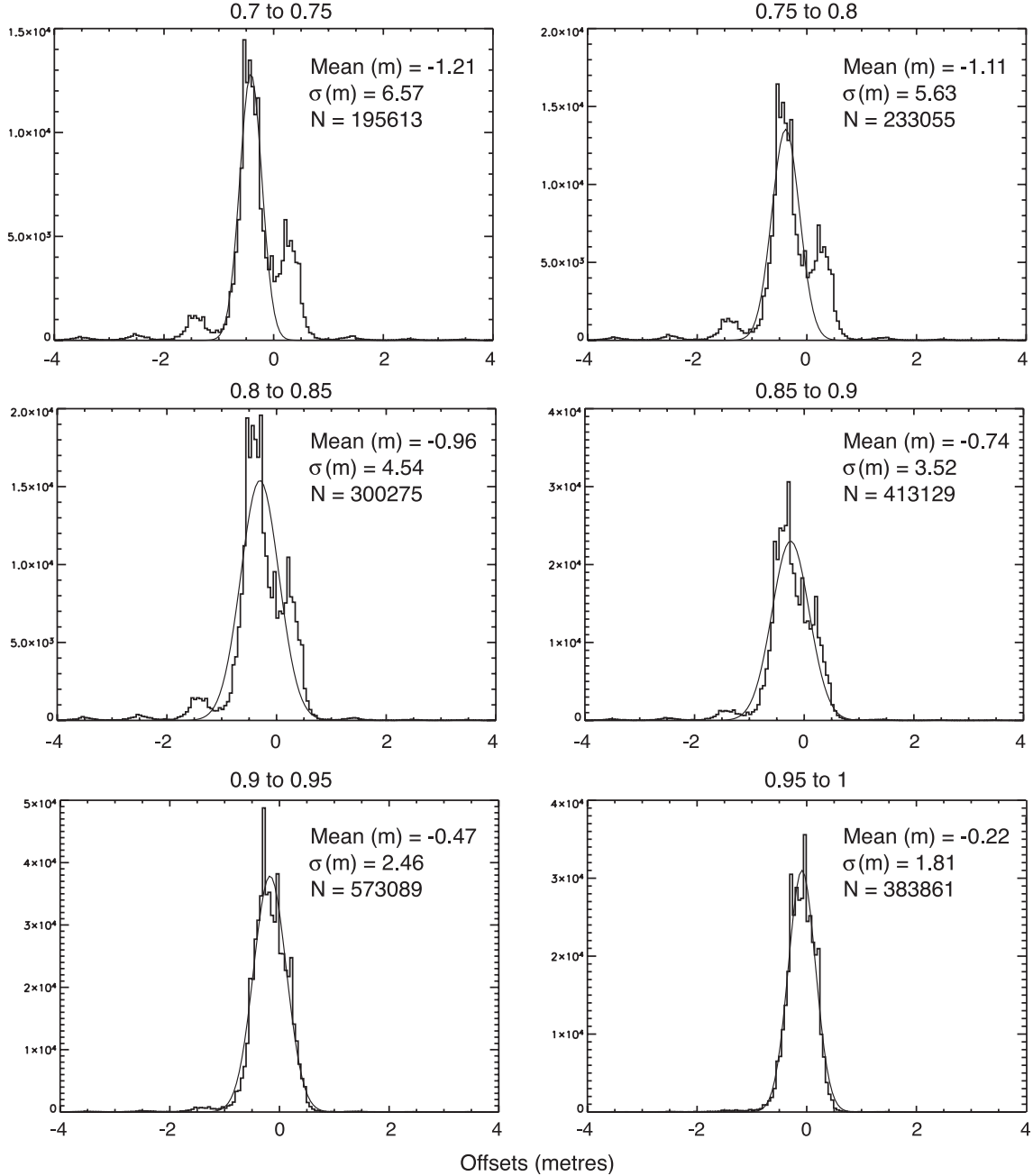


Fig. 6. Histograms of the residuals in the image line direction off the glaciers as a function of the correlation coefficient for image pair #2. The mean, the standard deviation (σ), and the number of points (N) of our distribution are indicated on each plot.

measured displacements (occurring in 21 to 28 days depending on the date of survey) are rescaled to the displacement (in meters) occurring during 26 days. This time interval was chosen because it is the duration of the SPOT orbital-repeat cycle. This rescaling implicitly assumes that the ice-velocity is constant.

4.3.1. The influence of changes in glacier elevation

In Fig. 8, we compare, along a longitudinal profile of the *Mer de Glace* glacier, the displacements in the column direction of the 19 July 2003 image derived from image pair #1 and from DGPS. Satellite measurements along a single

profile and the mean of five parallel profiles separated by 25 m are displayed. The small difference between these two data sets indicates that the short-wavelength noise is small. There is a clear systematic bias between the satellite and DGPS displacements. This bias, on the order of 1.5 m, is not observed in the direction of image lines.

This shift is the consequence of the non-vertical incidence angle of the satellite images (Table 1) combined with the strong ablation lowering the glacier surface during summer time. Fig. 9 illustrates this difference between measured and real displacements. Elevation changes, assumed to be equal to surface ablation for a short summer period, are estimated

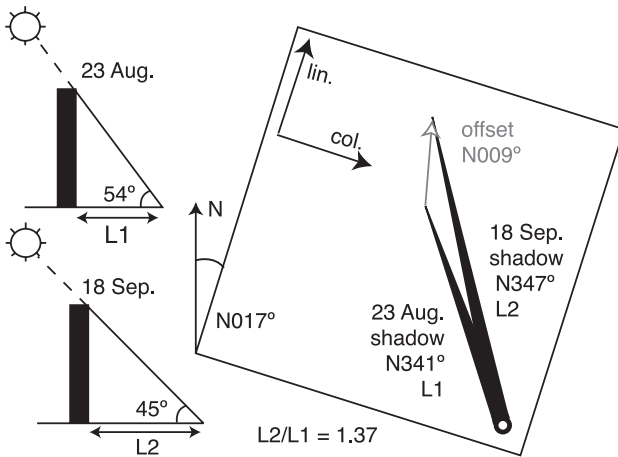


Fig. 7. Effect of the Sun's illumination angle on 23 August and 18 September 2003 on the length and orientation of the shadows. This effect explains why some unglacierized areas present, mostly in the image line direction, some negative residuals.

from a simple empirical degree-day model tuned with field measurements (Vincent, 2002). Each positive degree at a given altitude on the glacier yields an ablation of 6.6 mm of ice. The temperature is calculated from the records of the nearby Chamonix weather station assuming a constant adiabatic lapse rate of 6 °/km. Between 19 July and 19 August 2003, the estimated ablation is on the order of 3 m of ice at 1900 m on the glacier. Combined with the -24° incidence angle of the 19 July 2003 image, we calculate that our method overestimates the column offset by 1.3 m. This value is the same as the shift observed in Fig. 8. We account for this effect by modeling the ablation of the ice.

The correction is made by lowering, in the DEM, the surface of the glaciers with the estimated ablation. The correct ground position (λ_i, ϕ_s, z_s in Fig. 9) of the image point ($x + \Delta x, y + \Delta y$) is deduced from this corrected DEM. New values of the column displacements are obtained and added to Fig. 8 (grey triangles). This simple modelling corrects most of the systematic shift in the column displacements. The uncertainty of the estimation of the elevation change from the degree-day model is large, on the order of 30%. At 1900 m, it contributes ± 0.4 m of uncertainty to the column displacement measurement for image pair #1 and ± 0.13 m for image pair #2.

Pairs of images acquired with similar and large incidence angles could be used to measure precisely elevation change on glaciers, or more generally, on the Earth's surface. If the

magnitude or the direction of the ice flow is known accurately, the differences between the real and the satellite-derived column displacements could be converted to changes of elevation.

4.3.2. Accuracy of the satellite-derived displacements

Finally, we compare the DGPS and SPOT5-derived displacements. At the location of each stake, we extract the value of the displacements in column, line, and the correlation coefficient for each satellite image pair. Of the 29 stakes surveyed, 12 are located on the *Mer de Glace* glacier, and 17 on the *Argentière* Glacier. In Table 4, we present the results of the comparison. Some of the differences could result from the temporal mismatch between the dates of surveys (Fig. 4) and from the uncertainties in the DGPS measurements (± 21 cm). This table underlines the high accuracy obtained for both image pairs. As expected, the rms discrepancy is generally smaller for image pair #2 (on the order of 0.5 m in both image directions) than for image pair #1 (around 1 m). For all 29 stakes, the absolute differences between SPOT and DGPS displacements are on the order of 1/5 of the pixel size (0.5 m) except in the line direction for image pair #2. When considering each glacier independently, the results are slightly different.

For the *Mer de Glace* glacier, the most important differences appear in the line direction for image pair #2. We believe that this difference cannot be explained by an error in the satellite measurement and is, therefore, a real velocity change of the glacier. First, the accuracy is two times better for pair #2 than for pair #1, as shown by the standard deviations in Table 4. We also expect the displacements in the line direction to be the most accurate because the stereoscopic effect and errors due to ablation affect the column direction only. The “shadowing effect” described previously could explain a systematic error in the image line direction. But shadows are limited on glaciers and, if they were present, would lead to an apparent acceleration of the *Mer de Glace* glacier. These differences could result from a short-term velocity change of the *Mer de Glace* glacier discussed below.

4.4. Accuracy without GCPs and with a coarse DEM

As explained previously, our methodology can be applied without GCPs by skipping the step of the

Table 3

Mean and standard deviation (in parentheses), in meters, of the residuals off the glaciers for different correlation coefficients intervals

Image pair	0.7–0.75	0.75–0.8	0.8–0.85	0.85–0.9	0.9–0.95	0.95–1
#1	Col. 0.20 (12.34)	0.16 (10.46)	0.16 (8.27)	0.05 (6.32)	-0.10 (4.74)	-0.20 (4.24)
	Lin. -0.48 (14.04)	-0.41 (11.44)	-0.34 (8.40)	-0.21 (5.60)	-0.10 (3.28)	-0.02 (2.35)
#2	Col. -0.30 (5.33)	-0.31 (4.58)	-0.28 (3.68)	-0.23 (2.84)	-0.14 (1.96)	-0.06 (1.47)
	Lin. -1.21 (6.57)	-1.11 (5.63)	-0.96 (4.54)	-0.74 (3.52)	-0.47 (2.46)	-0.22 (1.81)

Residuals in column (Col.) and line (Lin.) directions for the two pairs of images are presented. Note that the standard deviations are roughly twice as small for image pair #2. Also, note the relation between the residuals in lines and the correlation coefficient caused by the “shadowing effect” (see text).

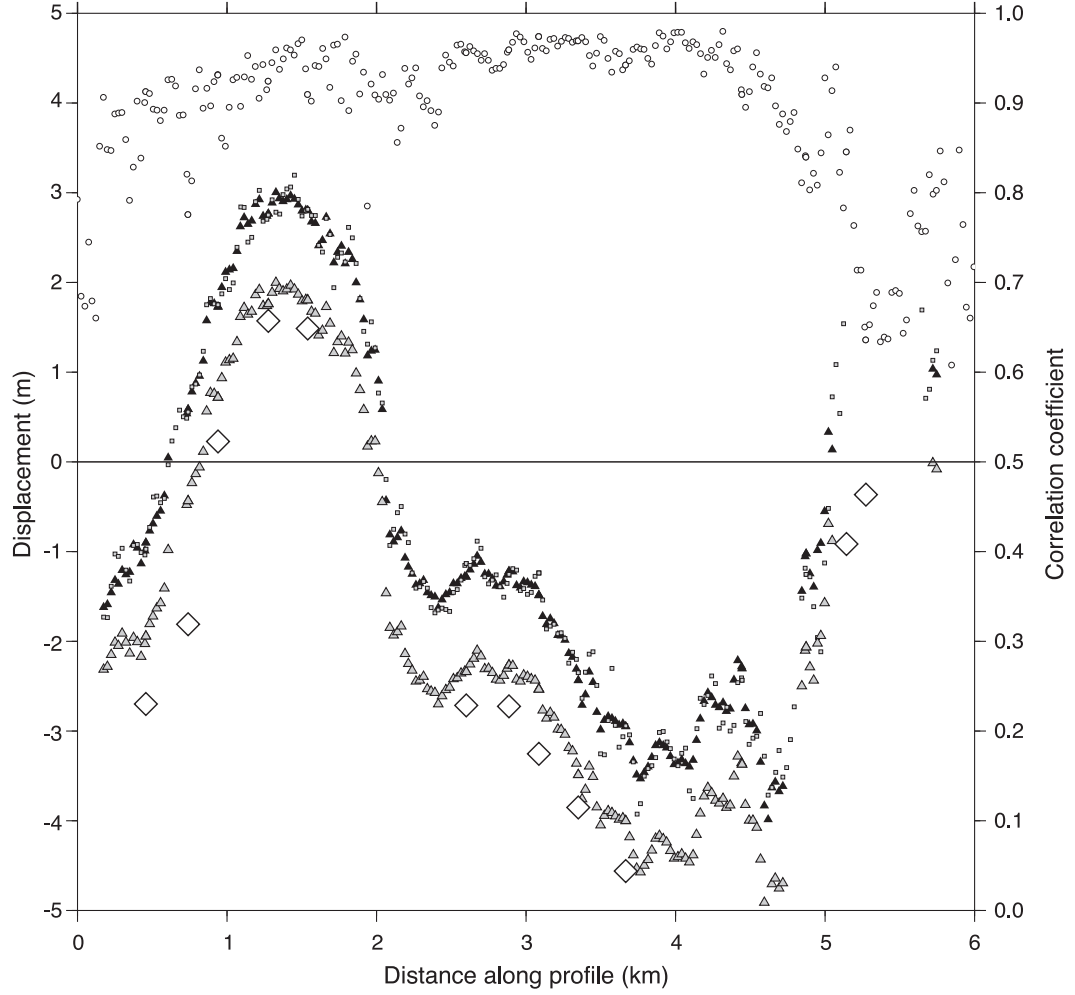


Fig. 8. Displacements along a longitudinal profile of the *Mer de Glace* glacier in the column image direction deduced from the 19 July and 19 August 2003 image pair. All displacements were rescaled to 26 days. The small light grey squares are the displacements from SPOT images along a single profile, whereas the black triangles represent the mean of 5 parallel profiles separated by 25 m. The white diamonds are the DGPS displacements. The black circles (filled in white) represent the correlation coefficient of the satellite measurement (right axis). The grey triangles represent the satellite displacements after correction for ablation.

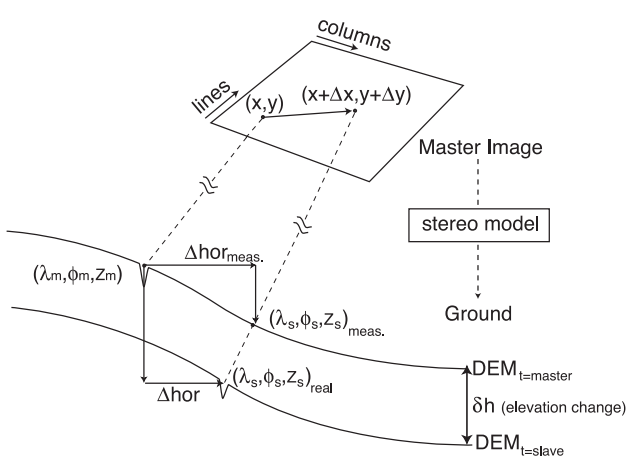


Fig. 9. Difference between the real and measured displacements caused by lowering of the glacier surface. This systematic error only affects measurements in the column direction.

absolute orientation. Consequently, we obtain two well coregistered images but with a shift relative to the DEM. The stereoscopic effect is less well modelled so that some distortions remain between the two images. We choose image pair #2 to test the accuracy obtained without GCPs because this pair presents a weak stereoscopic effect. The relative orientation of the two images is not significantly better with GCPs as shown in Table 2. The comparison with the DGPS survey (Table 4) confirms that accurate displacements can be obtained without GCPs. It is interesting to note that the difference is even smaller in some locations. We obtain a similar accuracy when using the GTOPO30 DEM (also without GCPs) instead of the high resolution DEM. It indicates that, with a good image pair, our methodology can be applied to remote areas where no high resolution DEM is available. The main limitation in using a coarse DEM is that elevation errors in the DEM, combined with non-

Table 4

Mean and standard deviation (in parentheses), in meters, of the difference between the displacements derived from SPOT5 images and measured during a differential GPS field campaign

Image pair	<i>Argentière</i>	<i>Mer de Glace</i>	All data
#1	Col.	0.38 (0.71)	0.6 (0.34)
	Lin.	0.65 (0.93)	0.39 (0.38)
#2	Col.	0.22 (0.47)	0 (0.4)
	Lin.	0.47 (0.53)	1.33 (0.46)
#2 no GCPs	Col.	0.28 (0.46)	0.01 (0.47)
	Lin.	0.52 (0.6)	1.2 (0.33)
#2 no GCPs	Col.	0.07 (0.43)	-0.35 (0.42)
GTOPO30	Lin.	0.54 (0.65)	1.29 (0.44)
			0.88 (0.67)

The offsets in columns (Col.) and lines (Lin.) for the two image pairs and also image pair #2 without GCPs (with the high resolution DEM and the GTOPO30 DEM) are presented.

vertical incidence angles, will result in georeferencing errors. They can lead to significant displacement errors in areas where the velocity gradient is large, which is

not the case near our DGPS surveys, located close to the glacier centerline.

4.5. A likely ice-acceleration event on the *Mer de Glace* glacier

Fig. 10 shows that a velocity change may affect that part of the *Mer de Glace* glacier located between the *Géant* icefall and its confluence with the *Leschaux* glacier. The mean velocity change between image pair #1 and #2 for this part of the profile is 12.6 m a^{-1} or 11.6% in 30 days. The DGPS velocities are even slightly greater than the one deduced from image pair #1, dating the ice-acceleration event in mid-August 2003. Such rapid summer velocity changes of glaciers have been reported previously. They are usually explained by higher sliding velocities due to higher basal water pressures (e.g., Mair et al., 2001). In early August 2003, a pronounced heat wave baked Europe, increasing the surface melting on glaciers in the Alps. This rapid water input could explain the increase in basal water pressure and sliding on part of the *Mer de Glace* glacier. In

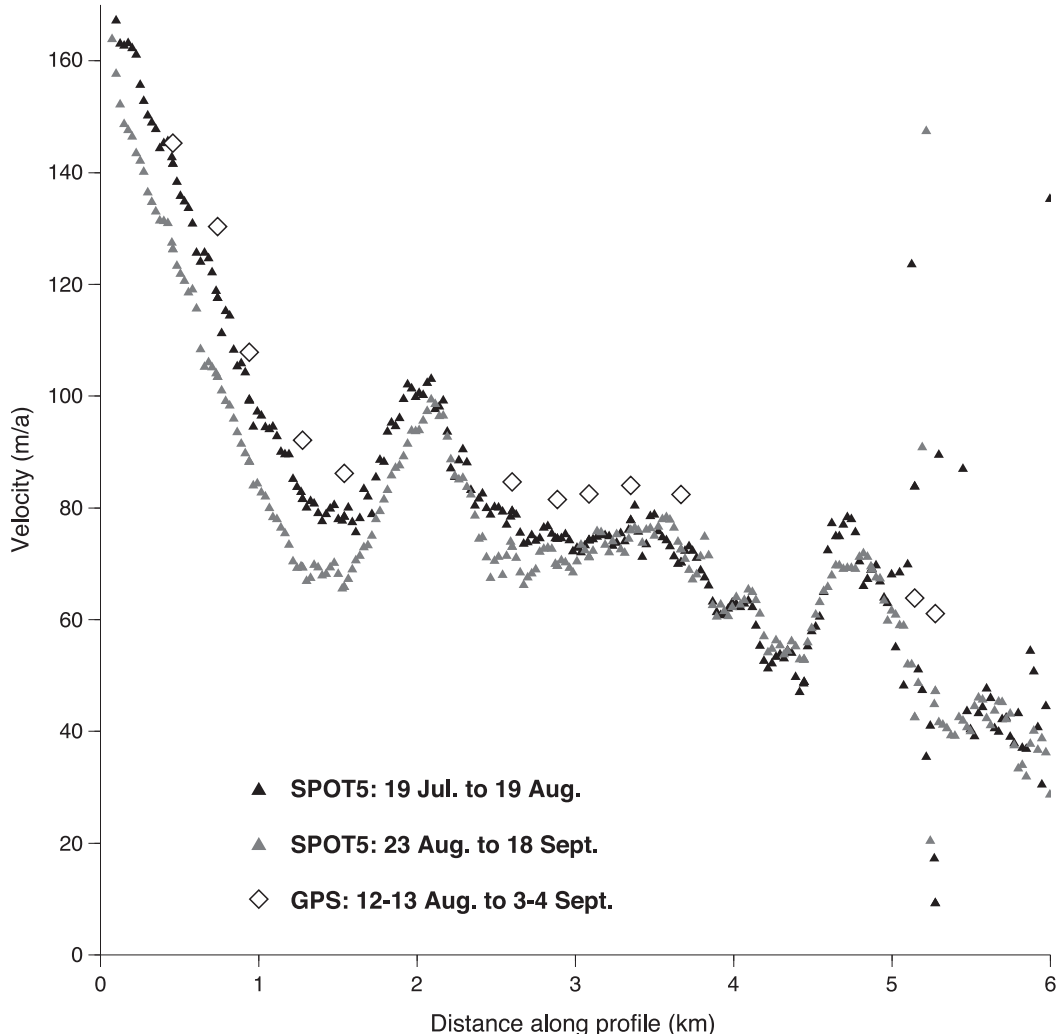


Fig. 10. Horizontal surface velocities along a longitudinal profile of the *Mer de Glace* glacier determined from satellite images and DGPS surveys.

future work, a more detailed study of the spatial pattern of the velocity change will help better understand the causes of this ice-acceleration event.

5. Conclusions

The goal of measuring displacements on mountain glaciers with an accuracy of one fourth the pixel size (0.62 m with SPOT5 images) has been achieved. The uncertainty in the DGPS survey (0.21 cm), the temporal mismatch between the ground surveys, and the acquisition dates of the SPOT5 images, combined with a sudden increase in ice-velocity prevent us from confirming definitively the accuracy from field observations. Yet, an uncertainty of 0.5 m in each image direction seems reasonable if satellite images are acquired from a similar point of view. This uncertainty of 0.5 m over 26 days is equivalent to 2 cm over 1 day, very close to the accuracy obtained from InSAR using ERS-1/ERS-2 tandem pairs. Our approach is accurate enough to measure a 10% velocity increase on the *Mer de Glace* glacier during and just after the pronounced heat wave in Europe in early August 2003.

Because our approach does not require GCPs, our methodology can be routinely and rapidly applied to new pairs of images. The high accuracy obtained without GCPs using the GTOPO30 DEM suggests the possibility of monitoring numerous glaciers, even in remote areas and without a contemporaneous DEM. The key step is the relative orientation of the two correlated images using precise homologous points. The accuracy of the measurement is controlled mainly by the radiometry (low gain is better for glaciers to avoid sensor saturation) and the geometry of the images. The “shadowing” effect, highlighted on the motionless area surrounding the glaciers, could be a problem for the applications other than glaciology. The rapidly changing elevation of mountain glaciers in summertime, because of ablation, can create a systematic error in the displacements along the image column direction. Addressing this issue, however, requires external information. This systematic bias could be used to monitor the elevation change of glaciers throughout the ablation season.

Images acquired from a similar point of view, with incidence angles differing only by a few degrees, are best. Vertical incidence eliminates the systematic errors caused by ablation but such a constraint also reduces the likelihood of obtaining two good images.

Among the limitations of our approach is that a velocity measurement during the summer may not be representative of the annual dynamics of a glacier. Thus, annual surveys of ablation stakes on a few glaciers are needed and complement the satellite-derived measurements. Another limitation is the difficulty in acquiring two cloud-free images with similar incidence angles.

Other geological phenomena that deforms the Earth's surface, such as earthquakes, landslides, and volcanoes

could also be surveyed using the cross-correlation of SPOT5 images. Depending on the expected direction of displacements, the incidence angles could be chosen for optimum accuracy. For mostly horizontal (respectively vertical) displacements, images with vertical (respectively oblique) incidence angles are preferable. For these applications other than glaciology, one interesting and promising topic to explore would be the fusion of displacements obtained by InSAR and optical image cross-correlation to obtain a 3-dimensional surface-displacement map.

Acknowledgments

Aurélie Bouilllon provided useful help concerning the SPOT5 algorithms. The comments of R. S. Williams Jr. and an anonymous reviewer led to significant improvements of the manuscript. We thank M. Bauer who provided valuable guidance as Editor-in-Chief. SPOT5 images were acquired thanks to the ISIS program (copyright CNES). This work was supported by the French national program ACI-OT Glaciers, the GDR STRAINSAR and the French GLACIO-CLIM program. The LGGE and IRD Great Ice Unit provided support for the field experiment. GMT software (Wessel & Smith, 1998) illustrated the article. The first author gratefully acknowledges a thesis fellowship from the French government.

References

- Al-Rousan, N., Cheng, P., Petrie, G., Toutin, T., & Valadan Zoej, M. (1997). Automated DEM extraction and orthoimage generation from SPOT level 1B imagery. *Photogrammetric Engineering and Remote Sensing*, 63, 965–974.
- Berthier, E., Arnaud, Y., Baratoux, D., Vincent, C., & Rémy, F. (2004). Recent rapid thinning of the “Mer de glace” glacier derived from satellite optical images. *Geophysical Research Letters*, 31(17) doi:10.1029/2004GL020706.
- Berthier, E., Raup, B., & Scambos, T. A. (2003). New velocity map and mass-balance estimate of Mertz Glacier, East Antarctica, derived from Landsat sequential imagery. *Journal of Glaciology*, 49(167).
- Braithwaite, R. J. (2002). Glacier mass balance: the first 50 years of international monitoring. *Progress in Physical Geography*, 26(1), 76–95.
- Centre National d'Etude Spatiale, (2002). MEDICIS software, distributed by CSSI.
- Ferrigno, J. G., & Williams, R. S., Jr. (1983). Limitations in the use of Landsat images for mapping and others purposes in snow- and ice-covered regions: Antarctica, Iceland and Cape Cod, Massachusetts. *International Symposium on Remote Sensing of Environment 17th, vol. 1*. (pp. 335–355) Ann Arbor, Michigan: Environmental Research Institute of Michigan.
- Fischer, A., Rott, H., & Björnsson, H. (2003). Observation of recent surges of Vatnajökull, Iceland, by means of ERS SAR interferometry. *Annals of Glaciology*, 37, 69–76.
- Fratter, D., Moulin, M., Ruiz, H., & Charvet, P. D. Z. (2001). The SPOT-5 mission. 52nd International Astronautical Congress. Toulouse, France.
- Frezzotti, M., Capra, A., & Vittuari, L. (1998). Comparison between glacier ice velocities inferred from GPS and sequential satellite images. *Annals of Glaciology*, 27, 54–60.

- Goldstein, R. M., Engelhardt, H., Kamb, B., & Frolich, R. M. (1993). Satellite radar interferometry for monitoring ice sheet motion: application to an Antarctic ice stream. *Science*, 262(5139), 1525–1530.
- Gray, A. L., Short, N., Mattar, K. E., & Jezek, K. C. (2001). Velocities and flux of the Filchner Ice Shelf and its tributaries determined from speckle tracking interferometry. *Canadian Journal of Remote Sensing*, 27(3), 193–206.
- Joughin, I. R., Kwok, R., & Fahnestock, M. A. (1998). Interferometric estimation of the three-dimensional ice-flow velocity vector using ascending and descending passes. *IEEE Transactions on Geoscience and Remote Sensing*, 36(1), 25–37.
- Kääb, A. (2002). Monitoring high-mountain terrain deformation from repeated air- and spaceborne optical data: examples using digital aerial imagery and ASTER data. *ISPRS Journal of Photogrammetry and Remote Sensing*, 57(1–2), 39–52.
- Kääb, A., Wessels, R., Haeberli, W., Huggel, C., Kargel, J., & Khalsa, S. (2003). Rapid ASTER imaging facilitates timely assessment of glacier hazards and disasters. *EOS, Transactions, Am. Geophys. Un.*, 84(13), 117–121.
- Lucchitta, B. K., & Ferguson, H. M. (1986). Antarctica: measuring glacier velocity from satellite images. *Science*, 234(4780), 1105–1108.
- Mair, D., Nienow, P., Willis, I., & Sharp, M. (2001). Spatial patterns of glacier motion during a high velocity event: Haut Glacier d’Arolla, Switzerland. *Journal of Glaciology*, 47(156), 9–20.
- Massonnet, D., & Feigl, K. (1998). Radar interferometry and its application to changes in the Earth’s surface. *Reviews of Geophysics*, 36(4), 441–500.
- Mattar, K. E., Vachon, P. W., Geudtner, D., Gray, A. L., Cumming, I. G., & Brugman, M. (1998). Validation of alpine glacier velocity measurements using ERS tandem-mission SAR data. *IEEE Transactions on Geoscience and Remote Sensing*, 36(3), 973–984.
- Mohr, J. J., Reeh, N., & Madsen, S. N. (1998). Three dimensional glacial flow and surface elevation measured with radar interferometry. *Nature*, 391(6664), 273–276.
- Paterson, W. S. B. (1994). The physics of glaciers (3rd edition). New York: Pergamon.
- Rabus, B., Eineder, M., Roth, A., & Bamler, R. (2003). The shuttle radar topography mission—a new class of digital elevation models acquired by spaceborne radar. *ISPRS Journal of Photogrammetry and Remote Sensing*, 57, 241–262.
- Rabus, R. T., & Fatland, D. R. (2000). Comparison of SAR-interferometric and surveyed velocities on a mountain glacier: Black Rapids Glacier, Alaska, U.S.A. *Journal of Glaciology*, 46(152), 119–128.
- Reynaud, L. (1980). Reconstruction of past velocities using Forbes bands (Mer de Glace). *Zeitschrift für Gletscherkunde und Glazialgeologie*, 15(2), 149–163.
- Rignot, E., Vaughan, D. G., Schmeltz, M., Dupont, T., & MacAyeal, D. (2002). Acceleration of Pine Island and Thwaites Glaciers, West Antarctica. *Annals of Glaciology*, 34, 189–194.
- Scambos, T. A., Dutkiewicz, M. J., Wilsoni, J. C., & Bindschadler, R. A. (1992). Application of image cross-correlation to the measurement of glacier velocity using satellite image data. *Remote Sensing of Environment*, 42(3), 177–186.
- SPOT-Image, (2002). SPOT Satellite Geometry Handbook, SNT-73_12-SI, Edition 1, Revision 0.
- Strozzi, T., Luckman, A., Murray, T., Wegmüller, U., & Werner, C. (2002). Glacier motion estimation using SAR offset-tracking procedures. *IEEE Transactions on Geoscience and Remote Sensing*, 40(11), 2384–2391.
- Toutin, T., & Cheng, P. (2002). A comparison of automated DEM extraction results using along-track ASTER and across-track SPOT stereo images. *Optical Engineering*, 41(9), 2102–2106.
- USGS, (1996). The GTOPO30 DEM. <http://edcdaac.usgs.gov/gtopo30/gtopo30.asp>
- Vadon, H., & Massonnet, D. (2000, 24–28 July). Earthquake displacement fields mapped by very precise correlation: complementary with radar interferometry. In I. Periodicals (Ed.), *IEEE International Geoscience and Remote Sensing Symposium. New Jersey* (pp. 2700–2702).
- Van Puymbroeck, N., Michel, R., Binet, R., Avouac, J. P., & Taboury, J. (2000). Measuring earthquakes from optical satellite images. *Applied Optics*, 39(20), 3486–3494.
- Vincent, C. (2002). Influence of climate change over the 20th century on four French glacier mass balances. *Journal of Geophysical Research*, 107(D19), 4375.
- Wessel, P., & Smith, W. H. F. (1998). New, improved version of generic mapping tools released. *EOS, Transactions, Am. Geophys. Un.*, 79(47), 579.